Landscape and Urban Planning 238 (2023) 104812

Contents lists available at ScienceDirect

Landscape and Urban Planning

journal homepage: www.elsevier.com/locate/landurbplan

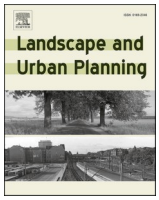

Urbanisation of a growing tropical mega-city during the 21st century — Landscape transformation and vegetation dynamics

Phakhawat Thaweepworadej [a,b], Karl L. Evans [a,*]

[a] Ecology and Evolutionary Biology, School of Biosciences, The University of Sheffield, Sheffield S10 2TN, UK
[b] Department of Biology, Faculty of Science, Mahidol University, Bangkok 10400, Thailand

HIGHLIGHTS

- Impervious surface cover increased in Bangkok by ~ 474 km^2 from ~ 2004 to ~ 2018.
- Space-for-time substitution approaches can predict future vegetation dynamics.
- ~583 km^2 of grassland and ~ 94 km^2 of rice-fields were lost; tree-cover grew by ~ 137 km^2.
- Expansion, not densification, drove these changes — raising heat stress & flood risk.
- Densification drove substantial tree-cover loss, reducing ecosystem services, & biodiversity.
- Schemes promoting urban growth through densification must increase tree protection.

ARTICLE INFO

Keywords:
Compact city
Greenspace
Housing
Urban gradient
Urban growth
Urban woodland

ABSTRACT

Fine scale spatial and temporal patterns in land-cover dynamics arising from rapid urbanisation of tropical regions are poorly understood. We quantify changes in landcover across the Bangkok region using high-resolution aerial imagery from ~ 2004 to ~ 2018 and address three questions: i) does urbanisation generate temporal shifts in the form of vegetation cover-urbanisation intensity relationships?, ii) do urban expansion and densification generate different vegetation dynamics?, iii) do net changes in vegetation cover and loss vary with urbanisation intensity? The form of vegetation cover-urbanisation intensity relationships exhibited negligible temporal variation, supporting the use of space-for-time substitution approaches for predicting future landcover dynamics. During our study period impervious surface cover increased by ~ 474 km^2 and there were net losses of grassland (~583 km^2) and rice-fields (~94 km^2), and a net gain in tree cover (~137 km^2). These changes have substantial implications for urban heat islands, flood risk and biodiversity. Urban expansion contributed more to vegetation dynamics than densification, partly because expansion impacted more land. Densification minimised loss of green-space, grasslands, and agriculture (rice-fields), but generated substantial local tree cover loss, which is critical to retain in highly urbanised areas. This contrasts with increasing tree cover elsewhere, including areas experiencing urban expansion. Trade-offs thus arise between impacts on different vegetation types when meeting the demand for tropical urban development through densification or expansion. Densification benefits most vegetation types but must be accompanied with tree protection and planting schemes to balance these trade-offs and minimise detrimental impacts of densification on people, ecosystem services and biodiversity.

1. Introduction

Urbanisation is rapidly transforming earth's terrestrial surface, with 0.6–1.3 million km^2 of rural land having a high probability of being converted into urban areas between 2015 and 2050 (Huang, Li, Liu, & Seto, 2019). Nearly half of this growth is predicted to occur in Asia (Huang et al., 2019), a region which already contains significant urban regions (e.g. 16 megacities, defined as cities with over 10 million inhabitants) even though most of the Asian human population still resides in rural areas (United Nations, 2019). South-east Asia has experienced one of the fastest rates of urbanisation within Asia (ASEAN, 2017; Hughes, 2017), especially in its mega-cities (Estoque & Murayama,

* Corresponding author at: Ecology and Evolutionary Biology, School of Biosciences, The University of Sheffield, Sheffield S10 2TN, UK.
E-mail addresses: Phakhawat.tha@mahidol.edu (P. Thaweepworadej), karl.evans@sheffield.ac.uk (K.L. Evans).

https://doi.org/10.1016/j.landurbplan.2023.104812
Received 8 February 2022; Received in revised form 13 May 2023; Accepted 21 May 2023
Available online 17 June 2023

2015; Richards, Passy, & Oh, 2017; Xu et al., 2019). This is a major factor driving biodiversity loss in the region (Sodhi, Koh, Brook, & Ng, 2004; Sodhi et al., 2010), with almost all of the region's urban areas overlapping with its four biodiversity hotspots (Güneralp & Seto, 2013). The impact of urbanisation on biodiversity hotspots in Southeast Asia is predicted to increase significantly, with the urbanised area of these hotspots projected to grow from approximately 27,000 km^2 in 2000 to nearly 100,000 km^2 in 2030 (Seto, Güneralp, & Hutyra, 2012).

Environmental impacts of urban expansion can arise directly through conversion of natural habitat of high biodiversity value, such as forest and wetland, or indirectly through loss of agricultural land—which is then replaced by clearance and conversion of natural vegetation types to create new farmland. These indirect impacts are often much greater than direct impacts (Song, Pijanowski, & Tayyebi, 2015; van Vliet, 2019). In southeast Asia, around 2.5 Mha of agricultural land was urbanised during 1992 to 2015, accounting for approximately 80% of the region's urban land expansion (Barbier, 2004; Kummer & Turner, 1994; van Vliet, 2019). Urbanisation thus contributes significantly to the impact of agricultural expansion on tropical deforestation (Geist & Lambin, 2002). Conversely, urban expansion can lead to gains in tree cover when urban management policies encourage urban forestry and planting of street trees, especially if the original landscape has limited tree cover (Díaz-Porras, Gaston, & Evans, 2014; Nowak, Noble, Sisinni, & Dwyer, 2001; Parris, 2016).

There is a clear need to understand landscape dynamics arising from urbanisation which are spatially and temporally variable (Estoque & Murayama, 2015; Schneider et al., 2015; Seto, Fragkias, Güneralp, & Reilly, 2011; Song et al., 2021). Studies to date have quantified how topography and proximity to currently urbanised areas and transport networks influence the probability of urban expansion (e.g. Song et al., 2015; Xu et al., 2019), and how urbanisation can proceed along a gradual transition of increasing anthropogenic alteration of landscapes, i.e. from forest, to agriculture to urban land (e.g. Lemoine-Rodriguez, MacGregor-Fors, & Muñoz-Robles, 2019). Adverse impacts of urban growth can be reduced by effective planning regulations that limit urban expansion and instead promote increasing urban intensity in already urbanised areas, i.e. urban densification (Broitman & Koomen, 2015). Such regulations are lacking, however, in much of the global south, including southeast Asian cities resulting in marked loss and degradation of surrounding agricultural and semi-natural land as cities expand (Chandan, Bharath, & Ramachandra, 2014; Srivanit, Hokao, & Phonekeo, 2012; Song et al., 2021).

Despite much interest and progress in understanding urban landscape dynamics there is limited knowledge of fine-scale spatial patterns of urban expansion, including which vegetation types are converted to urban land-covers, and how landscape dynamics vary depending on base-line levels of urbanisation. This is especially the case in rapidly urbanising regions. Here, as a case study, we focus on Bangkok, Thailand, which is located within the Indo-Burma biodiversity hotspot (Myers, Mittermeier, Mittermeier, Da Fonseca, & Kent, 2000). Bangkok is one of southeast Asia's rapidly growing mega-cities with population estimates of 6.4 million in 2000, increasing to 8.3 million in 2010 and 10.5 million in 2020 (United Nations, 2018).

Our overall objective is to quantify recent changes in landcover across the greater Bangkok region via landcover classification from high-resolution aerial imagery. We quantify temporal changes in landcover from ~ 2004 to ~ 2018. We contrast the impacts of urban densification and expansion on vegetation cover by assessing if newly urbanised areas (created by urban expansion) have different landcover change dynamics compared to areas experiencing urban densification. We then assess the spatial pattern of landcover across the rural to urban gradient, assessing if landcover changes have generated temporal shifts in the relationship between urbanisation intensity and coverage of specific vegetation types. We then quantify how temporal changes in landcover vary with the magnitude of urbanisation intensity. Finally, we quantify how changes in vegetation cover arising from conversion to impervious surfaces, and from impervious surfaces to vegetation vary along the gradient of urbanisation intensity. The resultant data inform understanding of environmental impacts of urban development in South-East Asia and help develop recommendations for minimizing adverse impacts of urban development.

2. Methods

2.1. Defining the study area

Our study area was delimited by a 70 km × 80 km rectangle (5,600 km^2) centred approximately on the centre of Bangkok; it covers Metropolitan Bangkok and neighbouring provinces, i.e., Samuth-Prakarn, Samuth-Sakorn, Nakorn-Pathom, Nontaburi and Pathumthani (Fig. S1). The size and location of this grid captures the substantial amount of urban land-cover within the region that extends beyond the official administrative city limits, whilst also incorporating parts of the rural landscape surrounding Bangkok. This thus enables us to contrast land-cover change in urbanised and more rural locations whilst providing a suitable baseline for assessing further future impacts of urbanisation.

2.2. Land cover classification

The sampling region was divided into 5,600 1 km × 1 km cells and a grid of 140,000 evenly spaced sampling points (25 per cell, i.e. one sampling point every 200 m) in ArcGIS using the UTM coordinate system. The habitat type at each sampling point was determined from high-resolution aerial imagery obtained via Google Earth (following Evans, Newson, and Gaston (2009)). High-resolution cloud free google earth images were selected that were centred on i) 2004 and ii) 2018. We used the cloud free image that was closest in time to our target year. Images used for the most recent time period were from 2017 or 2018 and for the 2004 sampling date 94% of grid cells were assessed using images taken within three years of the target year (Table S1). The remaining 6% of grid cells were all located far from the centre of Bangkok in mainly rural areas and the images available for these cells were from 2008 to 2013. Urban land cover in these grid cells was typically small (1st time period: 6.7%; 2nd time period (i.e. 2017/2018): 6.8%) and the difference in percentage urban land cover between two time periods was insignificant (matched pair *t*-test: $P = 0.137$; $n = 272$). Inclusion of these grid cells thus has negligible influence on our estimates of how urbanisation influences land-cover change.

Land cover type at each sampling point was classified into one of nine categories: i) impervious surface (i.e. buildings, roads, pavements etc.; which is one of the most frequently used urbanisation intensity metrics (Moll et al., 2019), ii) trees (including shrubs), iii) grasslands (aerial imagery did not enable us to consistently distinguish managed and unmanaged grasslands), iv) rice fields (the dominant form of agriculture in the Bangkok region (Song et al., 2021)), v) salt pans, vi) green roofs, vii) bare ground, viii) construction sites and ix) water bodies. These categories were selected to enable us to distinguish grey-space (i.e. urban land cover), green-space (i.e. vegetation) and blue-space (i.e. areas of water) whilst obtaining as much information as is feasible given image quality regarding the precise nature of landcover within these categories.

Images clearly enabled grassland to be distinguished from areas of trees and shrubs (identified by canopy shapes and generation of shade). Vegetated rice fields were distinguished from grassland by the lattice network of fields, and uniform lighter green colour compared to other vegetation. Flooded rice fields were distinguished from permanent open water by checking images taken at different points within the same focal year together with the lattice network of fields. Rice fields were distinguished from salt pans as the later only occur immediately next to the sea, are smaller than rice fields and never fully vegetated. Construction sites were distinguished from other areas of bare ground by the presence

of building equipment or partially constructed infrastructure. Other land-cover types (impervious surface, water bodies, and green roofs) were straightforward to classify.

To validate the accuracy of our sampling approach we compared land-cover estimates generated in 20 grid cells using sampling grids of 25 and 100 evenly spaced cells. We did so using two randomly selected cells from each of ten categories of impervious surface cover (0–10%, 11–20%, …, 91–100%; defined using data from the 25 sampling point grid and 2018 imagery). For all major land cover types (i.e. impervious surface, total green area, trees, grassland, and rice field), the estimates of percentage land cover type derived from the two different sampling strategies are strongly correlated with each other (correlation coefficients ≥ 0.90; $P < 0.0001$ in all cases; Table S2).

The accuracy of our classifications was further confirmed by comparing landcover classifications obtained from aerial imagery taken during our second time period (2017 or 2018) with ground-truthed landcover classifications in March–April 2018 (n = 1,355). These comprised 150 points located at the centre of 150 1 km × 1 km cells that were selected using random stratification across the rural to urban gradient, and an additional 1,205 sampling points that were selected haphazardly due to their location close to travel routes between the randomly selected cells. These comparisons revealed that classifications had at least 90% accuracy (some apparent inaccuracies will be due to genuine change) for almost all landcover types (Table S3), with the exceptions being bare ground (62.50% accuracy) and construction sites (77.8% accuracy). These landcover types are particularly likely to exhibit rapid genuine change (as bare ground becomes vegetated due to succession or conversion to a construction site; and as construction sites are turned to impervious surfaces). We thus assessed if changes at these sampling points were due to classification error or genuine change by assessing all available aerial imagery between the date of the original image and the date at which ground-truthing occurred. All discrepancies were due to genuine landcover change (Table S3) implying that there was 100% classification accuracy for bare ground and construction sites.

2.3. Data analyses

All analyses were performed in R version 4.1.2 (R Core Team, 2021). We excluded grid-cells with over 80% surface water cover as such cells contain an insufficient number of land-based sampling points with which to estimate changes in land-cover with sufficient precision; all analyses are thus based on 5,482 (97.9%) of our original 5,600 grid cells. We start by quantifying changes between ~ 2004 and ~ 2018 in the percentage cover of each of the nine landcover types and change in total green area (i.e. combining grasslands, rice fields and trees) using matched paired t-tests. Note that net change in vegetated area can be smaller than the sum of changes across vegetated landcover types as many of these changes will not result in the loss of green-space (e.g. grassland may be converted to trees). Only one sampling point (<0.001 %) was a green roof, and this habitat type was excluded from the calculation of total green-space as the ecology of green roofs is very different to other green-spaces occurring at ground level (Maclvor, 2016). We used the false discovery rate (FDR) method of Benjamini and Hochberg (1995) to correct for multiple testing and report the FDR corrected *P*-values ('p.adjust' function in *stats* package). We estimated the region's area lost/gained of each landcover type by multiplying percentage lost/gained with the total area of land within our sampling grids, i.e. 5,482 km^2.

There is likely to be substantial heterogeneity in landcover change within the Bangkok region, especially regarding changes in vegetation types, depending on the original intensity of urbanisation. Areas that have recently become urbanised due to urban expansion will, for example, tend to have different vegetation dynamics than areas which were originally urbanised but are experiencing densification (Parris, 2016). We define grid cells with at least 25% impervious surface cover as urbanised grid cells (following Bonnington, Gaston, and Evans. (2014)). We then conducted three sets of matched paired t-tests that compare changes in vegetation cover, in total and for each vegetation type, across our two time periods for i) grid cells that became urbanised between our two focal time periods (termed "Urban expansion"; 973 grid cells), ii) grid cells that were already urbanised in ~ 2004 but in which impervious surface cover increases by <10% points, e.g. from 25% to 30% (termed "Remain urban"; 910 grid cells), iii) grid cells that were already urbanised in ~ 2004 and in which impervious surface cover increases by at least 10% points, e.g. changed from 25% to 35% impervious surface cover (termed "Urban densification"; 761 grid cells), and iv) grid cells that remained rural (i.e. impervious surface < 25%) during ~ 2004 to ~ 2018 (termed "Remain rural"; 2,756 grid cells). Comparing the results of these analyses enables us to assess how urban expansion and urban densification differentially influence vegetation dynamics, by contrasting rural sites that are converted to urban areas with those that remain rural, and contrasting urban sites that experience densification with those that do not. These analyses exclude a small proportion of grid cells (n = 82; 1.5%) that were urban in 2004 but which lose some impervious surface and became rural in 2018. The FDR method was applied for multiple comparison and corrected *P*-values are reported.

Equivalent analyses conducted using 40% impervious surface as a threshold to define urbanised grid cells (rather than 25%) generated very similar results (see Fig. S2; Table S4). We also conducted equivalent analyses that uses a more extreme definition of urban densification, i.e. a 15% point (not 10%) increase in impervious surface cover (e.g. from 25% to 40% impervious surface), and equivalent changes in the definition of which grid cells remained urban. The direction and magnitude of change in vegetated land-cover types in cells that remain urban and experience urban densification obtained from this alternative approach (see Table S5) are very similar to those obtained when using a 10% threshold for defining urban densification (see Table 2), and have negligible impacts on our conclusions.

Table 1
Median, mean (±standard error) proportion of each landcover type in our two time periods ~ 2004 and ~ 2018, in 1 km × 1 km grid cells (n = 5,482). *P*-values of matched paired t-tests assessing the statistical significance of these changes were corrected using the false discovery rate (FDR) method ('p.adjust' function in *stats* package). Note that green roofs were only detect at one sampling point (<0.001% of the total).

Landcover type	~2004		~2018		Net area loss/gain (km^2)	Matched paired *t*-test results	
	Median	Mean ± s.e.	Median	Mean ± s.e.		*t*	*P*
Impervious surface	0.125	0.205 ± 0.003	0.235	0.292 ± 0.33	474.74	51.16	<2.2e–16
Green areas (total)	0.844	0.768 ± 0.003	0.714	0.670 ± 0.33	–540.52	–51.34	<2.2e–16
Trees	0.160	0.189 ± 0.002	0.200	0.214 ± 0.21	136.50	13.50	<2.2e–16
Grasslands	0.333	0.357 ± 0.003	0.208	0.251 ± 0.25	–582.74	–41.95	<2.2e–16
Rice fields	0.004	0.222 ± 0.004	0.000	0.205 ± 0.38	–94.29	–9.35	<2.2e–16
Salt pans	0.000	5.0e–4 ± 2.0e–4	0.000	4.0e–4 ± 0.002	–0.55	–2.23	0.029
Green roof	0.000	0.000 ± 0.00	0.000	1.1e–5 ± 1.1e–5	0.05	1.00	0.317
Bare ground	0.000	0.002 ± 0.07	0.000	0.331 ± 0.001	92.10	17.46	<2.2e–16
Construction sites	0.000	0.001 ± 0.06	0.000	0.053 ± 3.0e–4	–25.77	–7.46	1.4e–13
Water bodies	0.004	0.010 ± 0.20	0.004	0.104 ± 0.002	30.15	4.77	2.4e–6

Table 2
Median, mean (±standard error) proportion of each vegetation type in our two time periods ~ 2004 and ~ 2018, in 1 km × 1 km grid cells classified as cells that change from rural to urban over this time period (urban expansion; n = 973), remain rural (n = 2,756), experience urban densification (n = 761), and remain urban without experiencing densification (n = 910). *P*-values of matched paired t-tests assessing the statistical significance of these changes were corrected using the false discovery rate (FDR) method (p.adjust function in R).

Urbanisation category	~2004		~2018		Matched paired *t*-test results	
	Median	Mean ± s.e.	Median	Mean ± s.e.	*t*	*P*
Green area cover (all vegetation types)						
Urban expansion	0.833	0.830 ± 0.003	0.609	0.583 ± 0.004	–55.83	<2.2e–16
Remain rural	0.955	0.925 ± 0.002	0.880	0.865 ± 0.002	–28.12	<2.2e–16
Urban densification	0.560	0.537 ± 0.005	0.360	0.356 ± 0.005	–52.36	<2.2e–16
Remain urban	0.435	0.439 ± 0.006	0.440	0.426 ± 0.005	–0.91	0.363
Tree cover						
Urban expansion	0.182	0.212 ± 0.005	0.208	0.225 ± 0.004	2.84	0.005
Remain rural	0.136	0.178 ± 0.003	0.167	0.212 ± 0.003	12.72	<2.2e–16
Urban densification	0.200	0.202 ± 0.005	0.160	0.175 ± 0.004	–6.28	7.6e–10
Remain urban	0.160	0.180 ± 0.004	0.217	0.229 ± 0.004	12.80	<2.2e–16
Grassland cover						
Urban expansion	0.500	0.484 ± 0.007	0.261	0.281 ± 0.005	–32.87	<2.2e–16
Remain rural	0.320	0.365 ± 0.005	0.240	0.281 ± 0.004	–22.78	<2.2e–16
Urban densification	0.320	0.316 ± 0.006	0.160	0.171 ± 0.004	–30.42	<2.2e–16
Remain urban	0.208	0.234 ± 0.006	0.160	0.188 ± 0.005	–11.70	<2.2e–16
Rice field cover						
Urban expansion	0.000	0.133 ± 0.006	0.000	0.761 ± 0.004	–13.91	<2.2e–16
Remain rural	0.391	0.382 ± 0.006	0.360	0.372 ± 0.006	–3.24	0.001
Urban densification	0.000	0.184 ± 0.002	0.000	0.009 ± 0.001	–6.30	7.4e–10
Remain urban	0.000	0.143 ± 0.002	0.000	0.009 ± 0.001	–5.35	1.4e–7

We then assess if urbanisation have generated temporal shifts in the relationship between urbanisation intensity and total vegetation cover and each of the major types of vegetation cover (i.e. trees, grassland, and rice fields). We modelled the relationship between percentage total vegetation cover and impervious surface cover as these two variables are not simply the inverse of each other as three of our landcover classifications are neither green-space or impervious surface (i.e. bare ground, construction sites, and salt pans). We modelled the focal vegetation

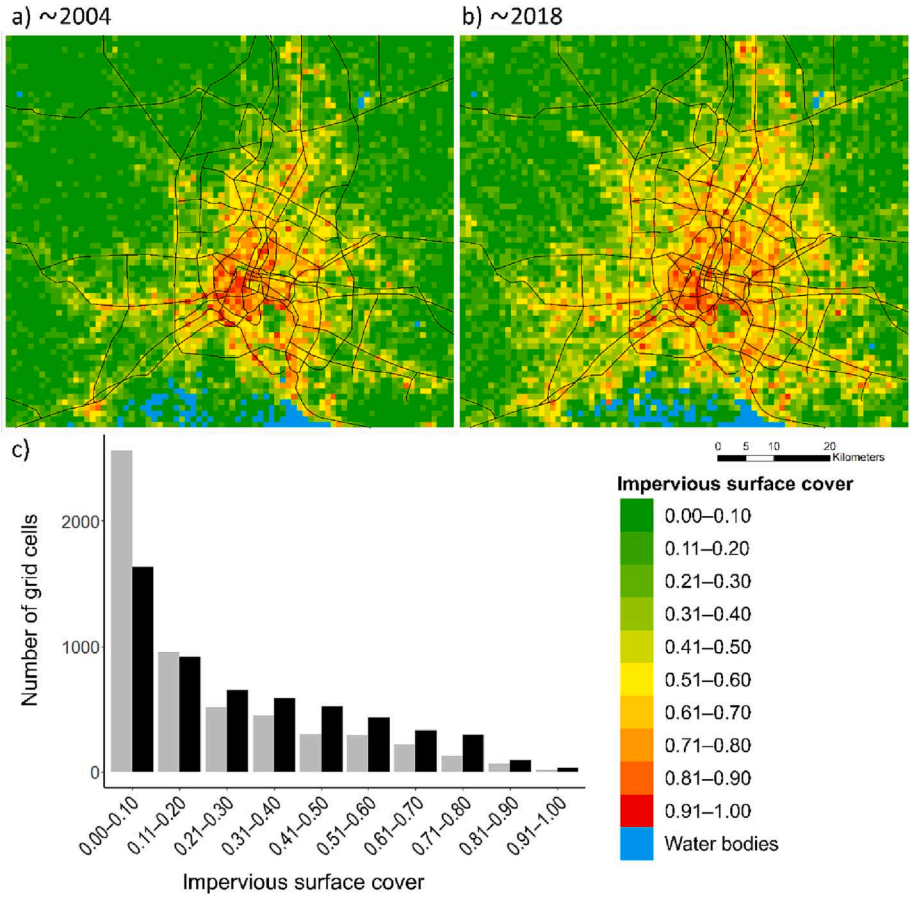

Fig. 1. Impervious surface cover across the Bangkok study region in a) ~ 2004 and b) ~ 2018, with lines representing major road networks, and c) number of 1 km × 1 km grid cells in each of the impervious surface categories in ~ 2004 (grey) and ~ 2018 (black). Note that much urban growth has arisen from urban sprawl, although urban densification is also occurring.

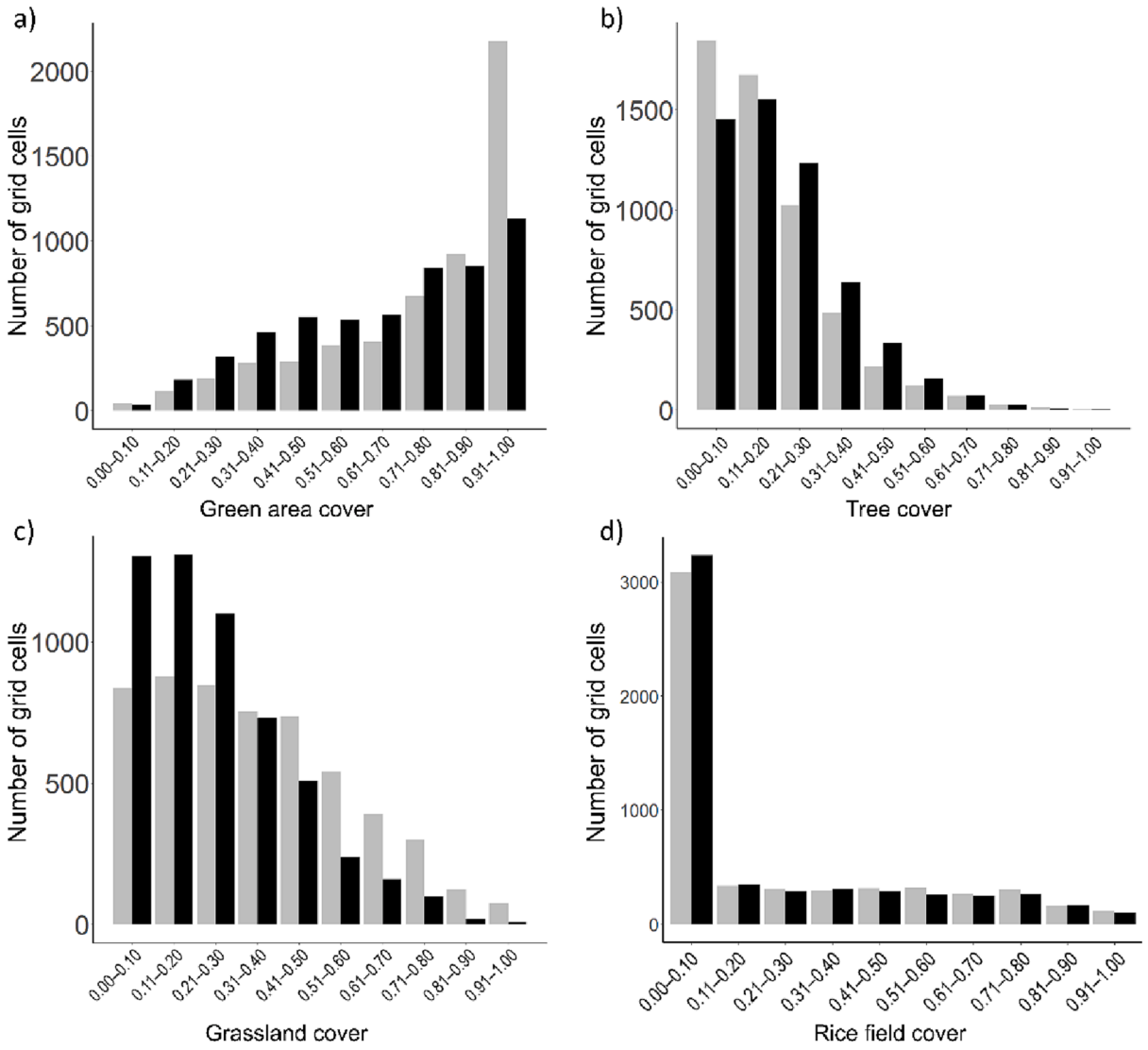

Fig. 2. Number of grid cells in each vegetated landcover category in ~ 2004 (grey) and ~ 2018 (black).

cover response variable as a function of the proportion of impervious surface (including linear, quadratic, and cubic terms to detect simple non-linear relationships) constructing separate models using data from each of our two time periods. We took this approach rather than fitting all data in the same model with additional predictors of time period and interaction terms between time period and urbanisation intensity due to the complexity of fitting and interpreting multiple interaction terms. Moran's I test (*ape* package) detected significant spatial autocorrelation for all our response variable/year combinations (Table S6). We thus constructed generalised least squared models ('gls' function in *nlme* package) using three different spatial correlation structure (exponential, spherical, or gaussian), selecting the optimal structure based on Akaike Information Criterion (AIC) values (Table S7). We selected models with higher power predictors only when their AIC values were $\geq$ 2 point values lower than alternative models, and when parameter estimates of the higher power predictors had 95% confidence intervals that did not overlap zero.

Finally, we calculated three measures of vegetation dynamics between our two time periods for each grid cell: i) total net loss/gain of total vegetation cover and each vegetation type, ii) loss of total vegetation cover and of each vegetation type arising from conversion to impervious surface cover, and iii) gain in total vegetation cover and each vegetation type arising from conversion of impervious surface cover to vegetation. This third type of vegetation dynamic is rare but can occur, for example, when an urban area is abandoned or when tree canopies expand. We then assess how vegetation dynamics change along the urbanisation gradient by modelling each type of vegetation dynamic as a function of impervious surface cover in our first time period whilst also taking into account the number of years between the two sets of images. We used linear, quadratic, and cubic terms of proportion of impervious surface, and again used AIC values, in combination with considering if 95% confidence intervals of parameter estimates overlap zero, to assess model fit. Moran's I tests (*ape* package) revealed positive spatial autocorrelation in our initial models' residuals (Table S8, S9), so we used generalised least squared model ('gls' function in *nlme* package) with three different spatial covariance structure (i.e., exponential, spherical, or gaussian) to take spatial correlation into account (Table S10).

3. Results

3.1. Summary of landcover transformations at the regional scale

From ~ 2004 to ~ 2018 there were significant gains in impervious surface (474.7 km^2) and tree cover (135.6 km^2), and significant losses of total vegetation cover (540.5 km^2), grassland (582.7 km^2) and rice fields (94.3 km^2) (Table 1; Fig. 2, Fig. 3). The net loss of total vegetation cover

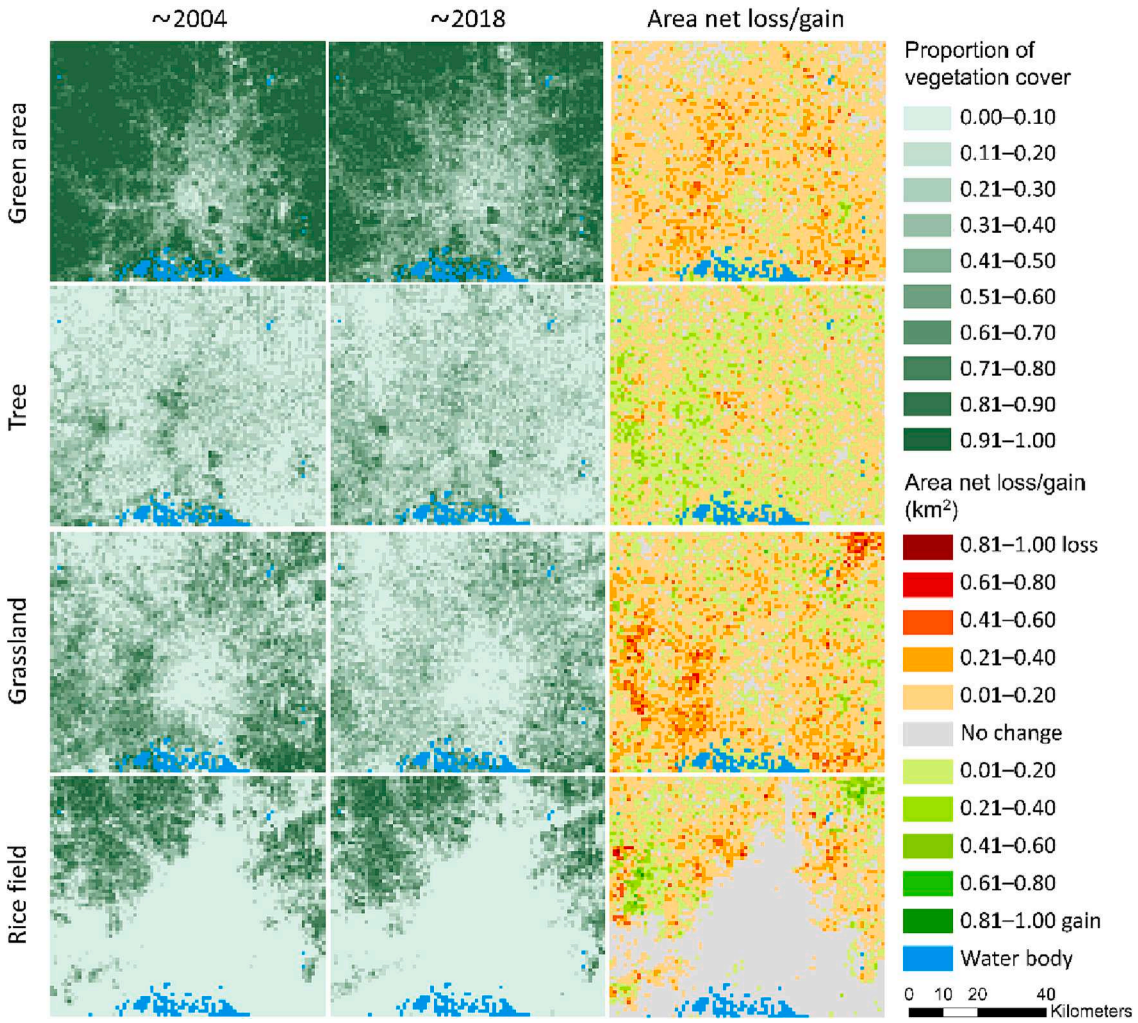

Fig. 3. Landcover maps show proportion of vegetation cover (total green area and three main vegetation types) of 1 km × 1 km grid cells in both time points and area net loss/gain (km^2) during ~ 2004 to ~ 2018. (For interpretation of the references to colour in this figure legend, the reader is referred to the web version of this article.)

is smaller than the sum of the area loss of each vegetation type due to dynamics across vegetation types, e.g. some grassland areas changed to tree-cover.

3.2. Impacts of urban expansion and densification on changes in vegetation cover

Despite the increase in impervious surface cover, our study region remained primarily rural (51.0% of grid cells met our definition of < 25% impervious surface cover). Approximately 18% of grid cells experienced urban expansion, with c. 14% experiencing urban densification (with mean impervious surface cover increasing from 42.5% to 62.1%; changes were similar when using a more conservative definition of intensification; Table S5), and c. 16% of cells were already urban but did not experience densification.

Total vegetation cover was substantially reduced in cells that experienced urban expansion and densification, declines were much smaller in cells that remained rural and there was no significant change in cells that remained urban (Table 2; Fig. 4a). Tree cover increased in all cell types, except those that experienced urban densification, where tree cover decreased (Table 2; Fig. 4b). Grassland cover declined in all cell types, including those that remained rural, with the smallest decline in cells that remained urban (Table 2; Fig. 4c). Rice field cover declined to a much greater extent in formerly rural grid cells that experienced urban expansion, than those that remained rural (Table 2; Fig. 4d). Change in rice field cover were negligibly elsewhere (Table 2; Fig. 4d). These patterns remain when using an alternative definition of urban densification of an increase of at least 15% points in impervious surface cover, with the exception of patterns in the amount of green-space in urban cells that did not experience densification switching from a pattern of no significant change to one of a slight reduction in the amount of green-space (Table S5).

3.3. Assessing temporal shifts in vegetation cover–urbanisation intensity relationships

Total vegetation cover declined linearly with increasing urbanisation intensity, and the gradient of these declines was extremely similar in both time periods (Table 3; Fig. 5a, e). Whilst tree cover–urbanisation intensity relationships changes from a cubic to a quadratic model, both models predicted that tree cover was maintained at approximately 25% until impervious surface cover reached approximately ~ 25%, after which tree cover declined linearly to negligible levels in the most intensely urbanised grid cells (Table 3; Fig. 5b, f). Grassland cover declined along cubic curves in both time periods with declines starting at very low levels of impervious surface cover and continuing to negligible levels once impervious surface cover reached 75% (Table 3; Fig. 5c, g), although in the first time period grassland cover is greater along much of

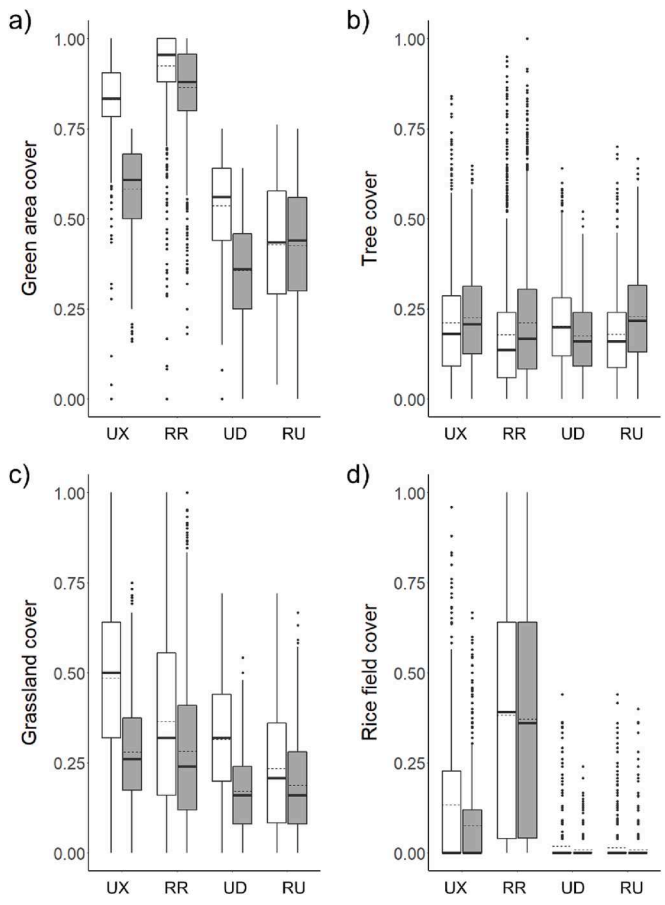

Fig. 4. Box and whisker plots comparing vegetation cover in ~ 2004 (white) and ~ 2018 (black) in each urbanisation category of 1 km × 1 km grid cells; urban expansion (UX), remain rural (RR), urban densification (UD), and remain urban (RU). Thick solid horizontal lines represent median, interquartile boxes represent middle 50% (25th to 75th percentile) of the data, and dashed lines represent mean values (on which matched paired t-tests are based; see Table 2), whiskers represent 25% ranges for the bottom and top of the data values, and dots represent outliers.

the urbanisation gradient. The area of rice fields declined along a cubic curve in both time periods with sharp reductions as urbanisation increased to approximately 25% impervious surface cover (Table 3; Fig. 5d, h). Consequently, there is limited evidence, for any vegetation type, that increasing urbanisation substantially changed the form of the relationship between green-space and urbanisation intensity.

3.4. Vegetation dynamics—net loss/gain along the urbanisation gradient

Change (i.e., net loss/gain) in total vegetation cover between the two time periods varied with initial urbanisation intensity along a positive slightly accelerating curve. The least urbanised cells lost the most vegetation cover, but when initial impervious surface exceeded 50% grid cells gained increasing amounts of vegetation cover between time periods (Fig. 6a).

Change in tree cover was positively and linearly associated with initial urbanisation intensity, such that the least urbanised areas have negligible gain in tree cover and the most urbanised cells gained the largest amount of tree cover (Table 4; Fig. 6b). Change in grassland cover exhibited a cubic relationship with initial urbanisation intensity (Table 4). The least urbanised locations in the first time period exhibited the largest losses in grassland cover, with the amount of grassland lost declining until initial impervious surface cover exceeded 70%, when cells gained grassland (Fig. 6c). Change in rice field cover exhibited a shallow linear relationship with initial impervious surface cover, with the largest (albeit still very limited) losses occurring in the least urbanised locations. In all these models the number of years between the first (~2004) and second images (~2018) was significantly negatively associated with change in total vegetation and grassland cover—indicating greater loss of these vegetation types as time progressed. Tree cover increases were larger as time progressed. These was no significant relationship between rice field net loss/gain and the number of years between the two images.

3.5. Vegetation dynamics—loss arising from conversion to impervious surface

Total vegetation loss arising from conversion to impervious surface cover declined with initial impervious surface cover along a slight unimodal curve (Table 5), with the greatest loss occurring when original impervious surface cover was approximately 25% (Fig. 7a). Loss of tree cover arising from conversion to impervious surface exhibited a cubic relationship with initial impervious surface cover (Table 5); the magnitude of change was limited across the gradient, being lowest at the highest levels of impervious surface cover and declining to negligible levels when impervious surface cover exceeds c. 70% (Fig. 7b). Grassland loss from conversion to impervious surface changed along a cubic curve with loss peaking at grid cells with approximately 20% impervious surface cover in 2004 then declining to negligible levels at the most urbanised locations (Fig. 7c). Rice field area loss due to conversion to impervious surface cover was negligible across the gradient but declined linearly with increasing urbanisation intensity (Fig. 7d). The amount of total vegetation, grassland, and rice fields, but not tree cover, loss due to conversion to impervious surface cover increased with time (Table 5).

3.6. Vegetation dynamics—gain arising from conversion from impervious surface

Gain in total vegetation cover and tree cover arising from conversion of impervious surface cover to green-space increased with initial impervious surface cover along a decelerating quadratic curve, which plateaued at ~ 50% impervious surface cover for total vegetation (Table 6; Fig. 7e) and at ~ 70% impervious surface cover for tree cover (Table 6; Fig. 7f). Gains in grassland area arising from conversion of impervious surfaces exhibited a unimodal relationship with initial impervious surface cover, with maximum gains at approximately 50% impervious surface and negligible gains at either extreme of the gradient (Table 6; Fig. 7g). There was no significant relationship between gain in rice fields and original urbanisation intensity (Table 6), although conversion of impervious surface to rice field is extremely rare (Fig. 7h; Fig. S3b).

4. Discussion

The Bangkok region has undergone intensive urbanisation during the focal study period, that has resulted in substantial loss of vegetation cover. The ultimate driver of this loss is increasing human population size (from 9.6 million in 2004 to 10.9 million in 2018; Bangkok Metropolitan Administration, 2018) and associated infrastructure development. There is substantial variation in trajectories of different vegetation types with substantial loss of grassland (582.7 km^2), more limited loss of rice fields (94.3 km^2), and tree cover increasing by 136.5 km^2. The increase in tree-cover in a region experiencing marked urbanisation is notable. It contrasts with frequent reports that tropical urbanisation drives loss of the urban forest (e.g. in Ghana, Tuffour-Mills, Antwi-Agyei, & Addo-Fordjour, 2020; Indonesia, Sejati, Buchori, & Rudiarto, 2018), but matches patterns reported in some areas of the global North (Díaz-Porras et al., 2014). This is probably a consequence of historical deforestation generating extremely limited tree cover in the agricultural land within the greater Bangkok area, combined with

Table 3

Parameter coefficients and standard errors of general least squared models ('gls' function in *nlme* package) with exponential spatial covariance structure that modelled total green area cover and cover of the three main vegetation types (i.e., trees, grassland, and rice fields) as a function of impervious surface cover in our two time periods (~2004 and ~ 2018) using linear, quadratic, and cubic models. Predicted values are illustrated in Fig. 5 derived from the best fitting model, identified in bold, i.e., that with the lowest AIC value in which 95% confidence intervals of all coefficients do not overlap zero.

Year	Response variable	Model	AIC	Intercept	Impervious surface cover (linear term)		Impervious surface cover (quadratic term)		Impervious surface cover (cubic term)	
				Coeff ± s.e.	Coeff ± s.e	95% CI (lower, upper)	Coeff ± s.e	95% CI (lower, upper)	Coeff ± s.e.	95% CI (lower, upper)
~2004	Green area cover	**Linear**	–15879.92	0.960 ± 0.006	–0.962 ± 0.006	–0.975, –0.950				
		Quadratic	–15874.99	0.962 ± 0.006	–0.984 ± 0.013	–1.010, –0.958	0.032 ± 0.018	–0.002, 0.067		
		Cubic	–15870.70	0.961 ± 0.006	–0.962 ± 0.022	–1.006, –0.918	–0.052 ± 0.071	–0.191, 0.088	0.074 ± 0.061	–0.045, 0.193
	Tree cover	Linear	–8173.25	0.237 ± 0.021	–0.221 ± 0.013	–0.246, –0.197				
		Quadratic	–8338.09	0.217 ± 0.022	0.093 ± 0.027	0.041, 0.146	–0.470 ± 0.036	–0.540, –0.400		
		Cubic	–8342.25	0.213 ± 0.022	0.201 ± 0.046	0.111, 0.290	–0.879 ± 0.145	–1.163, –0.595	0.321 ± 0.124	0.118, 0.604
	Grassland cover	Linear	–5742.53	0.454 ± 0.027	–0.493 ± 0.016	–0.524, –0.462				
		Quadratic	–5760.65	0.444 ± 0.027	–0.344 ± 0.034	–0.410, –0.278	–0.221 ± 0.045	–0.309, –0.134		
		Cubic	–5829.05	0.432 ± 0.028	0.045 ± 0.057	–0.066, 0.155	–1.708 ± 0.179	–2.059, –1.356	1.310 ± 0.153	1.010, 1.611
	Rice field cover	Linear	–6442.84	0.259 ± 0.043	–0.242 ± 0.015	–0.271, –0.212				
		Quadratic	–6727.25	0.289 ± 0.043	–0.713 ± 0.031	–0.773, –0.652	0.701 ± 0.040	0.621, 0.780		
		Cubic	–6852.43	0.303 ± 0.044	–1.182 ± 0.051	–1.282, –1.082	2.498 ± 0.162	2.180, 2.815	–1.584 ± 0.138	–1.855, –1.313
~2018	Green area cover	**Linear**	–15469.94	0.936 ± 0.009	–0.939 ± 0.006	–0.951, –0.928				
		Quadratic	–15467.48	0.939 ± 0.009	–0.969 ± 0.013	–0.995, –0.943	0.040 ± 0.016	0.008, 0.072		
		Cubic	–15466.49	0.941 ± 0.009	–1.014 ± 0.024	–1.061, –0.966	0.194 ± 0.072	0.053, 0.335	–0.129 ± 0.059	–0.244, –0.014
	Tree cover	Linear	–8511.35	0.288 ± 0.022	–0.278 ± 0.011	–0.299, –0.256				
		Quadratic	–8718.95	0.255 ± 0.023	0.057 ± 0.025	0.008, 0.105	–0.449 ± 0.030	–0.508, –0.390		
		Cubic	–8719.66	0.251 ± 0.023	0.143 ± 0.045	0.055, 0.231	–0.748 ± 0.133	–1.009, –0.488	0.251 ± 0.109	0.038, 0.464
	Grassland cover	Linear	–7257.15	0.366 ± 0.023	–0.386 ± 0.012	–0.410, –0.362				
		Quadratic	–7297.76	0.348 ± 0.023	–0.208 ± 0.028	–0.264, –0.152	–0.238 ± 0.034	–0.305, –0.171		
		Cubic	–7350.98	0.334 ± 0.024	0.115 ± 0.051	0.015, 0.215	–1.355 ± 0.150	–1.650, –1.060	0.935 ± 0.123	0.694, 1.176
	Rice field cover	Linear	–7182.49	0.272 ± 0.045	–0.265 ± 0.012	–0.289, –0.241				
		Quadratic	–7594.96	0.322 ± 0.046	–0.781 ± 0.027	–0.835, –0.728	0.691 ± 0.033	0.626, 0.755		
		Cubic	–7705.16	0.342 ± 0.048	–1.215 ± 0.048	–1.310, –1.120	2.191 ± 0.143	1.911, 2.471	–1.254 ± 0.116	–1.483, –1.026

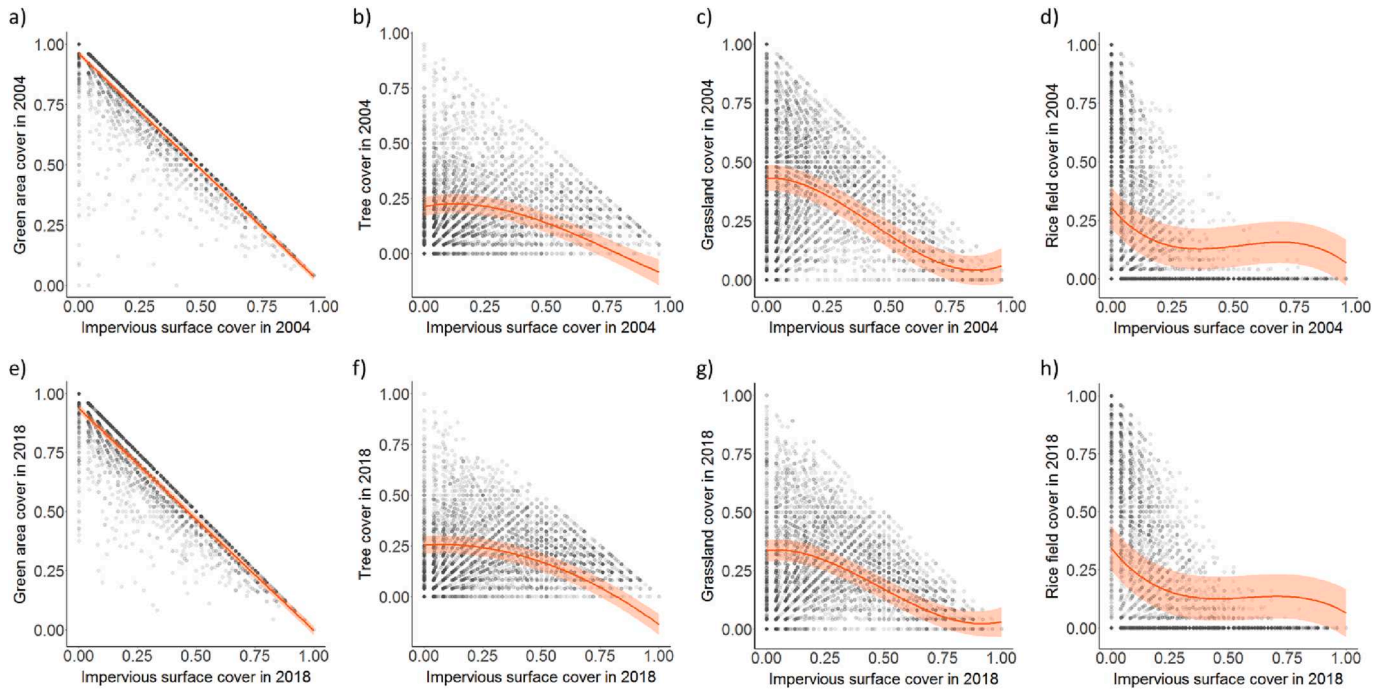

Fig. 5. Relationships between the proportions of total vegetation cover and each of three main vegetation types (tree, grassland, and rice field) and impervious surface cover in ~ 2004 (a-d) and ~ 2018 (e-h). Fitted lines represent predicted values from the best fit spatial models ('gls' function in *nlme* package) reported in Table 2.

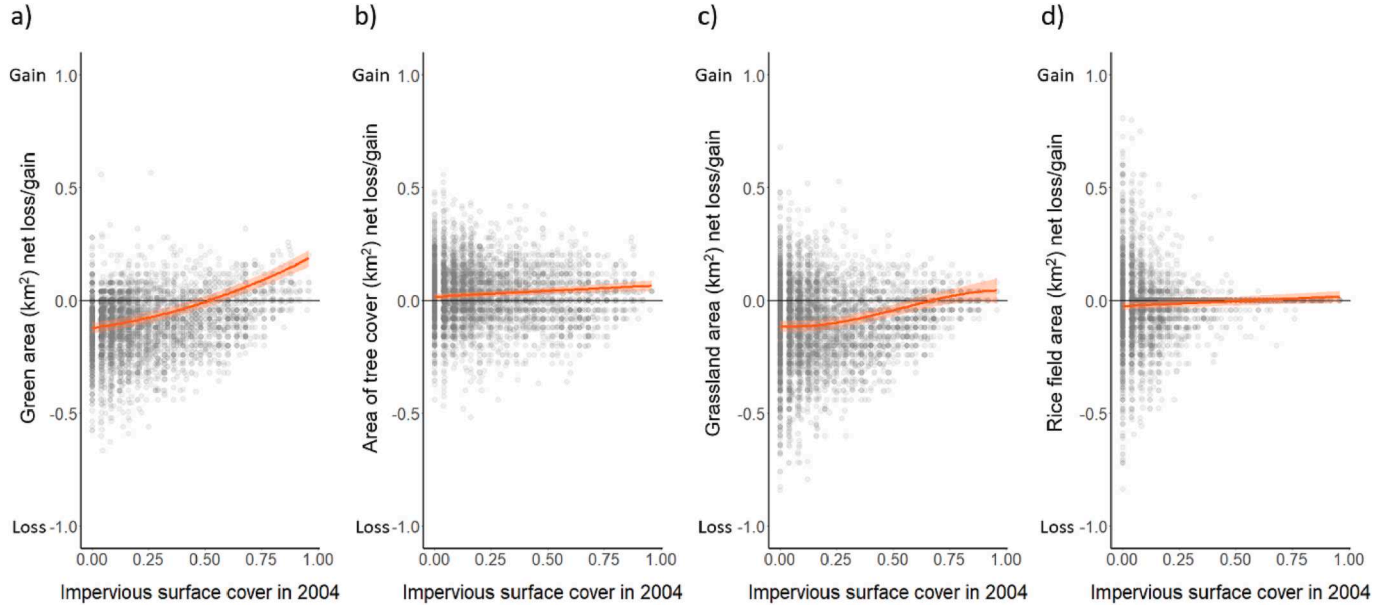

Fig. 6. Relationships between estimated area (km^2) net loss/gain of total green area (a) and three main vegetation types (b-d) during ~ 2004 to ~ 2018 with proportion of impervious surface in ~ 2004. Fitted lines illustrate predicted values and shading their 95% confidence intervals, derived from the best fitting spatial models ('gls' function in *nlme* package) presented in Table 4. (For interpretation of the references to colour in this figure legend, the reader is referred to the web version of this article.)

investment in urban tree planting (Thaiutsa, Puangchit, Kjelgren, & Arunpraparut, 2008).

4.1. Impacts of urban expansion and densification on vegetation dynamics

Quantifying the contribution of urban expansion and densification on these regional landcover transitions is dependent on the precise definitions used. Using different thresholds to define urbanised grid cells (i.e. 25% or 40% impervious surface) and alternative densification definitions (i.e., 10% or 15% points increase in impervious surface) generates similar patterns of vegetation cover change. Expansion and densification have divergent impacts on vegetation dynamics. Although declines of vegetation cover in grid cells that experienced expansion were approximately equally to those that experienced densification (~20%; Table 2), area of vegetation cover loss to urban expansion

Table 4
Parameter coefficients and standard errors from generalised least squares models ('gls' function in *nlme* package) with exponential spatial covariance structure that model area net loss/gain of total vegetation cover and the three main vegetation types (trees, grasslands, and rice fields) as a function of original impervious surface cover (i.e., in ~ 2004 with linear, quadratic, cubic terms) and number of years between the images. The best fitting models (assessed by AIC values and parameter estimates' 95% confidence intervals not overlapping zero) are shown in bold. Predicted values are illustrated in Fig. 5.

Response variable	Model	AIC	Intercept	Impervious surface cover (linear term)		Impervious surface cover (quadratic term)		Impervious surface cover (cubic term)		Numbers of year between image	
			Coeff ± s.e.	Coeff ± s.e.	95% CI (lower, upper)	Coeff ± s.e.	95% CI (lower, upper)	Coeff ± s.e.	95% CI (lower, upper)	Coeff ± s.e.	95% CI (lower, upper)
Green area net loss/gain	Linear	–9153.24	−0.026 ± 0.027	0.267 ± 0.011	0.245, 0.289					–0.008 ± 0.002	–0.011, –0.004
	Quadratic	–9181.39	0.135 ± 0.025	0.196 ± 0.033	0.087, 0.183	0.196 ± 0.033	0.132, 0.261			–0.007 ± 0.002	–0.011, –0.004
	Cubic	–9178.63	–0.017 ± 0.027	0.089 ± 0.043	0.006, 0.173	0.368 ± 0.135	0.103, 0.633	–0.152 ± 0.116	–0.379, 0.075	–0.007 ± 0.002	–0.011, –0.004
Area of tree cover net loss/gain	**Linear**	–8619.20	–0.054 ± 0.024	0.052 ± 0.011	0.030, 0.074					0.005 ± 0.002	0.002, 0.008
	Quadratic	–8620.87	–0.050 ± 0.024	–0.016 ± 0.026	–0.066, 0.035	0.101 ± 0.035	0.034, 0.169			0.005 ± 0.002	0.002, 0.008
	Cubic	–8618.43	–0.052 ± 0.024	0.035 ± 0.045	–0.053, 0.123	–0.091 ± 0.143	–0.371, 0.189	0.170 ± 0.122	–0.070, 0.409	0.005 ± 0.002	0.002, 0.008
Grassland area net loss/gain	Linear	–6173.16	–6.4e–5 ± 0.035	0.165 ± 0.015	0.136, 0.194					–0.009 ± 0.002	–0.014, –0.004
	Quadratic	–6183.21	–0.007 ± 0.035	0.047 ± 0.033	–0.017, 0.111	0.177 ± 0.043	0.092, 0.262			–0.009 ± 0.002	–0.014, –0.004
	Cubic	–6185.78	0.011 ± 0.035	–0.069 ± 0.056	–0.178, 0.041	0.616 ± 0.177	0.268, 0.963	–0.387 ± 0.152	–0.685, –0.090	–0.009 ± 0.002	–0.014, –0.004
Rice field area net loss/gain	**Linear**	–9324.70	0.026 ± 0.027	0.041 ± 0.011	0.019, 0.063					–0.004 ± 0.002	–0.007, 2.4e–4
	Quadratic	–9324.97	0.022 ± 0.027	0.100 ± 0.024	0.052, 0.148	–0.088 ± 0.032	–0.151, –0.024			–0.004 ± 0.002	–0.007, 2.1e–4
	Cubic	–9321.18	0.021 ± 0.027	0.129 ± 0.042	0.047, 0.210	–0.197 ± 0.132	–0.456, 0.062	0.097 ± 0.113	–0.125, 0.318	–0.004 ± 0.002	–0.007, 2.2e–4

Table 5
Parameter coefficients and standard errors from generalised least squares models ('gls' function in *nlme* package) with exponential spatial covariance structure that model loss of total vegetation cover and cover of three main vegetation types (trees, grasslands, and rice fields) arising from conversion of impervious surface in relation to original impervious surface cover (i.e., in ~ 2004 with linear, quadratic, cubic terms) and number of years between images. The best fitting models (assessed by AIC values and parameter estimates' 95% confidence intervals not overlapping zero) are shown in bold. Predicted values are illustrated in Fig. 6.

Response variable	Model	AIC	Intercept	Impervious surface cover (linear term)		Impervious surface cover (quadratic term)		Impervious surface cover (cubic term)		Numbers of year between image	
			Coeff ± s.e.	Coeff ± s.e.	95% CI (lower, upper)	Coeff ± s.e.	95% CI (lower, upper)	Coeff ± s.e.	95% CI (lower, upper)	Coeff ± s.e.	95% CI (lower, upper)
Green area loss to impervious surface	Linear	–12023.50	0.026 ± 0.024	–0.075 ± 0.009	–0.092, –0.058					0.006 ± 0.001	0.003, 0.008
	Quadratic	–12295.73	0.009 ± 0.024	0.211 ± 0.019	0.175, 0.248	–0.422 ± 0.025	–0.471, –0.374			0.005 ± 0.001	0.003, 0.008
	Cubic	–12294.12	0.007 ± 0.024	0.259 ± 0.032	0.197, 0.322	–0.605 ± 0.102	–0.805, –0.406	0.162 ± 0.087	–0.009, 0.332	0.005 ± 0.001	0.003, 0.008
Area of tree cover loss to impervious surface	Linear	–18813.19	0.020 ± 0.015	–0.009 ± 0.004	–0.018, –4.8e–4					0.001 ± 0.001	−0.001, 0.001
	Quadratic	–19037.82	0.012 ± 0.017	0.129 ± 0.010	0.110, 0.148	–0.205 ± 0.013	–0.231, –0.180			0.001 ± 0.001	−0.001, 0.002
	Cubic	–19043.53	0.014 ± 0.018	0.080 ± 0.017	0.047, 0.114	–0.021 ± 0.055	–0.129, 0.086	–0.163 ± 0.047	–0.255, –0.071	0.001 ± 0.001	−0.001, 0.002
Grassland area loss to impervious surface	Linear	–15185.08	0.013 ± 0.016	–0.045 ± 0.006	–0.058, –0.032					0.003 ± 0.001	0.001, 0.005
	Quadratic	–15340.59	0.004 ± 0.015	0.120 ± 0.014	0.092, 0.148	–0.243 ± 0.019	–0.280, –0.207			0.003 ± 0.001	0.001, 0.005
	Cubic	–15351.38	0.001 ± 0.015	0.200 ± 0.024	0.153, 0.247	–0.546 ± 0.077	–0.697, –0.395	0.267 ± 0.066	0.138, 0.397	0.003 ± 0.001	0.001, 0.005
Rice field area loss to impervious surface	**Linear**	–23055.13	–0.007 ± 0.007	–0.016 ± 0.003	–0.022, –0.010					0.002 ± 4.8e–4	0.001, 0.003
	Quadratic	–23050.00	–0.006 ± 0.007	–0.029 ± 0.007	–0.043, –0.016	0.019 ± 0.009	0.001, 0.038			0.002 ± 4.8e–4	0.001, 0.003
	Cubic	–23044.24	–0.007 ± 0.007	–0.018 ± 0.012	–0.042, 0.005	–0.022 ± 0.038	–0.097, 0.053	0.036 ± 0.033	–0.028, 0.101	0.002 ± 4.8e–4	0.001, 0.003

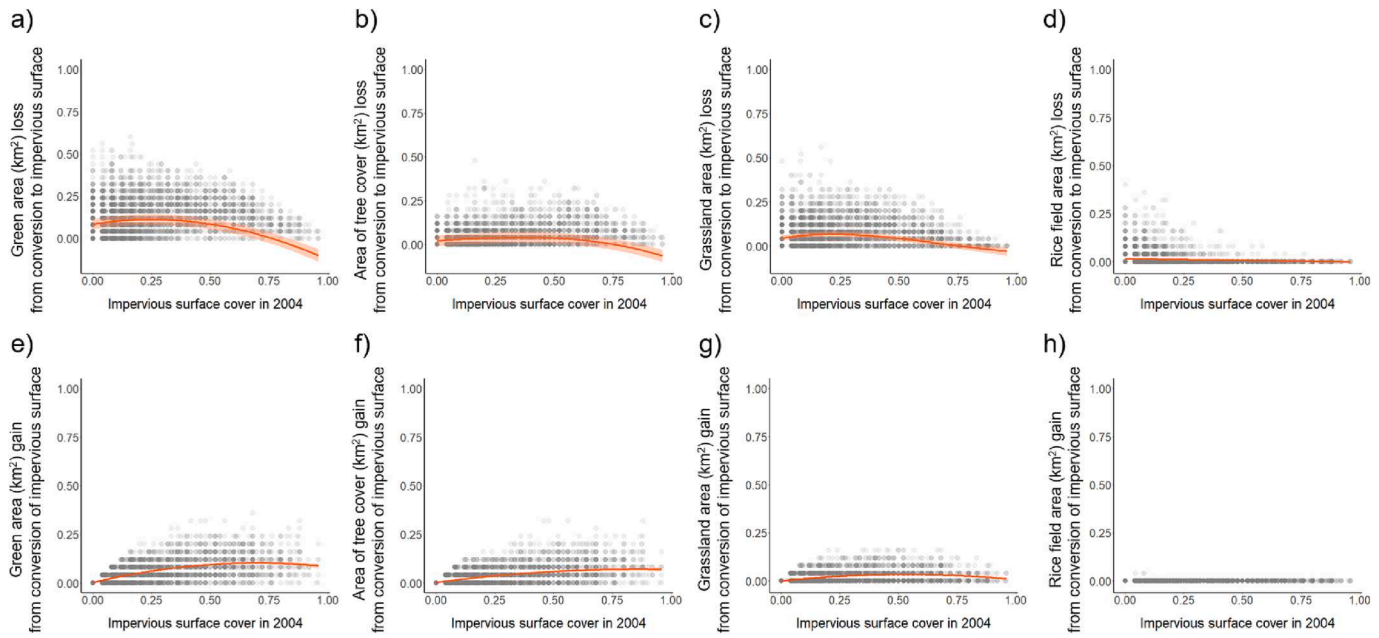

Fig. 7. Relationships between estimated loss of vegetation cover arising from conversion to impervious surface (a) total vegetation, (b) trees, (c) grasslands, and (d) rice fields, and gain of vegetation cover arising from conversion of impervious surface to vegetation surface (e) total vegetation, (f) trees, (g) grasslands, and (h) rice fields from ~ 2004 to ~ 2018 as a function of proportion impervious surface cover in ~ 2004. Fitted lines illustrate predicted values and shading their 95% confidence intervals, from the best fitting spatial models ('gls' function in *nlme* package) reported in Table 5 (panels a-d) and Table 6 (panels e-h); no best fitted line is illustrated in panel h due to the lack of a significant relationship.

(~240.7 km^2) was nearly double the loss from densification (~137.8 km^2) due to differences in the spatial extent of these processes. These losses were mainly driven by the conversion of grasslands, and again expansion resulted in almost twice as much grassland being lost than densification (expansion ~ 197.7 km^2, densification ~ 110.1 km^2). This is consistent with previous studies of urbanisation of South-East Asian megacities (Estoque & Murayama, 2015; Song et al., 2021; Xu et al., 2019). Greater adverse effects of urban expansion on vegetation cover may be particularly detrimental for conservation as expansion is more likely to impact semi-natural grasslands that occur in such locations rather than the more intensely managed grasslands within urban locations that are often of limited biodiversity value (Norton et al., 2019; Round & Gardner, 2008).

Densification is more likely to occur in urban grid cells with relatively large amount of vegetation cover, as such locations have more space for infill development. Despite this vegetation cover in the second time period (i.e. ~2018) was lower in cells with densification compared to other urbanised areas that did not experience densification. This confirms that a compact city approach to urban development that aims to reduce land consumption could profoundly adversely influence the amount and accessibility of urban green-spaces, leading to negative environmental consequences and implications for the quality of urban life (Haaland and van den Bosch, 2015; Pauleit, Ennos, & Golding, 2005).

Urban expansion resulted in the loss of approximately half the original cover of rice fields in these cells (equating to a loss of ~ 55.7 km^2), which is much greater than the loss arising from densification (~7.0 km^2)—primarily because rice fields are extremely rare in urban areas. Adverse impacts on food production are likely to be relatively small, however, given that losses from expansion equate to just 4.7% of the total area of rice fields (~1,148.0 km^2) within the study area at the start of our study period. Consequently, indirect effects of urbanisation on the conversion of natural forest to replace loss of agricultural land (Song et al., 2015; van Vliet, 2019) is rather limited within our study region, partly because much urban growth occurs through densification rather than expansion.

Densification resulted in a decline of ~ 20.8 km^2 of tree cover, yet tree cover increased in all other locations including those that experienced urban expansion (~12.6 km^2 increase). Our results contrast with previous suggestions that urban densification generates no net loss of tree cover as loss is balanced out by newly created tree cover (Kaspar, Kendal, Sore, & Livesley, 2017). The increases in tree cover that occur are likely to arise from growth of existing trees' canopies (Fig. S4), woodland succession over vacant lands (Fig. S5), creation of urban wooded habitat such as woodland blocks in parks, and tree planting in agricultural land and streets trees (partially a consequence of tree planting campaigns in the 1990s; Thaiutsa, Puangchit, Kjelgren, & Arunpraparut, 2008; Fig. S6).

4.2. *Temporal shifts in vegetation dynamics along the urbanisation gradient*

Generally, we found no strong evidence for temporal shifts in the form of vegetation cover-urbanisation intensity relationships between our focal time periods. This suggests that landcover patterns along the spatial urbanisation gradient in Bangkok are broadly constant, indicating the general ability of space-for-time substitution approaches (*sensu* Pickett, 1989) to predict future landcover change arising from urbanisation at least over the c. 15 year time period captured by out study. A slight shift in the form of grassland cover-urbanisation intensity relationships during our study period, arising from a substantial reduction in grassland cover, especially at the low levels of urbanisation intensity, suggest that the value of space-for-time substitution approaches may, however, vary between vegetation types. The predictive capacity of space-for-time substitution approaches can also be reduced by changes in urban planning or policy. As an example, whilst our data suggest that rice fields have been less impacted by urbanisation in recent decades in the Bangkok region, this seems likely to change due to a decision to construct a new airport and associated urban infrastructure in Bang Len district (the rural areas at the northwest corner of our study region; Hongtong, 2019) which is currently dominated by rice fields (Fig. S7). Further research that assesses spatial configuration of the

Table 6
Parameter coefficients and standard errors from generalised least squares models ('gls' function in *nlme* package) with exponential spatial covariance structure that model gain of total vegetation cover and cover of three main vegetation types (trees, grasslands, and rice fields) arising from conversion of impervious surface in relation to original impervious surface cover (i.e., in ~ 2004 with linear, quadratic, cubic terms) and number of years between images. The best fitting models (assessed by AIC values and parameter estimates' 95% confidence intervals not overlapping zero) are shown in bold. Predicted values are illustrated in Fig. 7.

Response variable	Model	AIC	Intercept	Impervious surface cover (linear term)		Impervious surface cover (quadratic term)		Impervious surface cover (cubic term)		Numbers of year between image	
			Coeff ± s.e.	Coeff ± s.e.	95% CI lower, upper	Coeff ± s.e.	95% CI lower, upper	Coeff ± s.e.	95% CI lower, upper	Coeff ± s.e.	95% CI lower, upper
Green area converted from impervious surface	Linear	–19393.07	0.003 ± 0.007	0.149 ± 0.004	0.141, 0.156					0.001 ± 0.001	–4.0e–4, 0.002
	Quadratic	–19649.18	–0.003 ± 0.007	0.285 ± 0.009	0.267, 0.303	–0.204 ± 0.012	–0.228, –0.179			3.5e–4 ± 4.8e–4	–0.001, 0.001
	Cubic	–19644.19	–0.003 ± 0.007	0.301 ± 0.016	0.269, 0.333	–0.263 ± 0.052	–0.365, –0.162	0.053 ± 0.044	–0.034, 0.140	3.5e–4 ± 4.8e–4	–0.001, 0.001
Area of tree cover converted from impervious surface	Linear	–21471.56	0.001 ± 0.006	0.097 ± 0.003	0.091, 0.104					4.0e–4 ± 4.4e–4	–4.7e–4, 0.001
	Quadratic	–21538.78	–0.002 ± 0.006	0.157 ± 0.008	0.142, 0.172	–0.092 ± 0.010	–0.112, –0.071			2.9e–4 ± 4.4e–4	–0.001, 0.001
	Cubic	–21532.23	–0.002 ± 0.006	0.162 ± 0.014	0.136, 0.189	–0.110 ± 0.043	–0.196, –0.025	0.017 ± 0.037	–0.056, 0.089	2.9e–4 ± 4.0e–4	–0.001, 0.001
Grassland area converted from impervious surface	Linear	–24788.49	0.003 ± 0.004	0.047 ± 0.002	0.043, 0.052					1.3e–4 ± 3.1e–4	–4.7e–4, 0.001
	Quadratic	–25017.29	–0.001 ± 0.004	0.124 ± 0.005	0.114, 0.135	–0.117 ± 0.007	–0.132, –0.103			8.3e–5 ± 2.6e–4	–4.2e–4, 0.001
	Cubic	–25011.44	–0.001 ± 0.004	0.134 ± 0.010	0.115, 0.154	–0.155 ± 0.031	–0.217, –0.094	0.033 ± 0.027	–0.019, 0.086	7.9e–4 ± 2.6e–4	–4.3e–4, 5.8e–4
Rice field area converted from impervious surface	Linear	–60847.87	2.7e–4 ± 8.3e–5	–3.4e–5 ± 5.8e–5	–1.5e–4, 7.9e–5					–1.8e–5 ± 6.2e–6	–3.0e–5, –6.0e–6
	Quadratic	–60831.09	2.7e–4 ± 8.3e–2	–2.7e–5 ± 1.8e–4	–3.7e–4, 3.2e–4	–1.1e–5 ± 2.5e–4	–4.9e–4, 4.7e–4			–1.8e–5 ± 6.2e–6	–3.0e–5, –6.0e–6
	Cubic	–60817.56	2.6e–4 ± 8.3e–5	1.9e–4 ± 3.5e–4	–5.0e–4, 8.7e–4	–0.001 ± 0.001	–0.003, 0.001	0.001 ± 0.001	–1.2e–3, 2.6e–3	–1.8e–5 ± 6.2e–6	–3.1e–5, –6.1e–6

mosaic of green and grey spaces is required to address fully how changes in urban landscapes influence vegetation cover and associated ecological features, for example spatial patterns depicted in Fig. 1 indicate that urban sprawl along some road networks is fragmenting some large blocks of green-space that were previously well connected to rural areas.

4.3. Implications for ecosystem function and tropical biodiversity

We find that space-for-time substitution approaches are likely to be valid for projecting future impacts on vegetation dynamics of the projected future increases in urbanisation within the Bangkok region (Song et al., 2021). The trend of increasing impervious surface cover and associated declines in vegetation cover are thus highly likely to continue, enhancing the urban heat islands (Morabito et al., 2021), which increased from 12.7 °C in 2005 to 16.2 °C in 2016 (Khamchiangta & Dhakal, 2020). Increased impervious surface cover and reduced vegetation cover will also increase surface water runoff (Ramamurthy & Bou-Zeid, 2014), which combined with the flat lowland geography of the Bangkok region (Thanvisitthpon, Shrestha, & Pal, 2018) and projected precipitation increase (Cooper, 2019) will substantially increase flood risk. Recent flooding events in Bangkok, especially the 2011 floods, had major economic and human well-being impacts (Poapongsakorn & Meethom, 2013).

The notable increase in tree cover, contrasting with the loss of shorter vegetation in grasslands and rice fields, could potentially mitigate some of the adverse impacts on regulation of air temperature and flood risk (Lin et al., 2021). This mitigation potential will be enhanced by the fact that tree cover gain has been greatest in locations that were highly urbanised at the start of our study period. Despite this, newly created urban tree cover may not always provide equivalent ecosystem services and functions to the original vegetation (Wang, Zhou, Wang, & Qian, 2019), and urban densification resulted in significant loss of tree cover. There is thus likely to be significant fine scale spatial variation in how the land-cover dynamics we document influence ecosystem service provision, which requires further investigation.

Biodiversity will also be significantly impacted by the land-cover changes that we document, with urbanisation and increasing impervious surface cover associated with reduced avian, squirrel and tree species richness including in the Bangkok region (Thaweepworadej & Evans, 2022a; Thaweepworadej & Evans, 2022b; Thaweepworadej & Evans, 2022c). These adverse impacts can partially be mitigated by increasing urban tree-cover, at least for avian species (Thaweepworadej & Evans, 2022a). There will thus also be local scale variation in biodiversity responses to urban land-cover change, with avian biodiversity in areas experiencing urban densification being particularly adversely impacted via their greater loss of tree cover. Grassland specialists are typically particularly negatively influenced by urbanisation intensity (Lakatos, Chamberlain, Garamszegide, & Batáry, 2022) and subsequently are frequently rare in urban areas (Jones & Bock, 2002), except those that can tolerate frequently mown short grassland. The loss of grassland cover may further the already documented decline of these species in Bangkok (Round & Gardner, 2008). Seasonal flooded rice fields, whilst contributing largely to regional food production, can also support biodiversity depending on the magnitude of pesticide use (e.g. plants—Kamoshita, Arai, & Nguyen, 2014), birds—Angkaew et al., 2022), fish—Cochard, Maneepitak, and Kumar, 2014, and arthropods—Cochard, Maneepitak, and Kumar, 2014). Although areas of rice field loss reported in this study was relatively small—~94.3 km^2, conversion of such habitats, could substantially reduce freshwater biodiversity.

4.4. Impacts of development policies

Thailand's land code allows the Department of Lands (Thailand) to file a petition to cancel the owner's land right if land is unused for over five consecutive years (for lands under a certificate of utilisation) or over

ten years for lands under a title deed (Thailand. Ministerial Regulation, 1954). Such regulation is likely to encourage land-use patterns that halt vegetation succession and promote conversion of semi-natural vegetation to alternative land-uses. There is thus considerable value in assessing the potential to redefine land-use under the act to include the provision of ecosystem services from green-space as a legitimate land-use. Perhaps more positively in 2022 the Bangkok governor launched the One-million-trees campaign aiming to plant an additional million trees in the Bangkok Metropolitan region (Sittipunt, 2022), which comprises approximately 25% of our study region. Our data provide a useful baseline to assess the impact of this policy on changes in urban tree-cover, which could mitigate impacts of densification on tree-cover, and the extent to which other forms of green-space are lost to accommodate intensive tree planting.

5. Conclusions

Using classification of high-resolution aerial imagery, our study documents that intensive urbanisation in the Bangkok region during the first part of the 21st century has generated a profound loss of vegetation cover, although there was considerable variation across vegetation types. Despite this, the form of spatial patterns of vegetation cover along the gradient of urbanisation intensity appears to largely be invariant in time, indicating the ability of space-for-time substitution approaches to predict future vegetation dynamics. At the scale of individual grid cells, changes in total vegetation and grassland cover arising from urban densification and expansion are similar, but expansion has generated much greater losses then densification as it has occurred across a much larger area. Loss of rice fields is relatively small but has primarily arisen from expansion. Conversely, densification has generated substantial loss of tree cover contrasting with gains in tree cover throughout the rest of the region. The loss of such trees is likely to be particularly important for biodiversity, and provision of ecosystem services as their provision typically scales with vegetation biomass, and demand for such services is often greatest in the most urbanised locations. There is potential to reduce environmental impacts of the continuing demand for additional urban land in the Bangkok region by promoting densification above expansion. Such an approach will, however, require active promotion of tree retention and planting schemes to avoid detrimental impacts on people and biodiversity.

CRediT authorship contribution statement

Phakhawat Thaweepworadej: Conceptualization, Methodology, Formal analysis, Investigation, Data curation, Writing – original draft, Visualization. **Karl L. Evans:** Conceptualization, Methodology, Writing – review & editing, Supervision.

Declaration of Competing Interest

The authors declare that they have no known competing financial interests or personal relationships that could have appeared to influence the work reported in this paper.

Data availability

Data will be made available on request.

Appendix A. Supplementary data

Supplementary data to this article can be found online at https://doi.org/10.1016/j.landurbplan.2023.104812.

References

Angkaew, R., Round, P. D., Ngoprasert, D., Powell, L. A., Limparungpatthanakij, W. Y., & Gale, G. A. (2022). Collateral damage from agricultural netting to open-country bird populations in Thailand. *Conservation Science and Practice*.

Associations of Southeast Asian Nations (ASEAN). (2017). *Celebrating ASEAN: 50 years of evolution and progress, a statistical publication*. Statistics Division: The ASEAN Secretariat.

Bangkok Metropolitan Administration, Administrative Strategy Division. (2018). *Statistical profile of Bangkok Metropolitan Administration*. (in Thai) Available from: http://www.bangkok.go.th/pipd/page/sub/16726/.

Barbier, E. B. (2004). Explaining agricultural land expansion and deforestation in developing countries. *American Journal of Agricultural Economics, 86*(5), 1347–1353.

Benjamini, Y., & Hochberg, Y. (1995). Controlling the false discovery rate: A practical and powerful approach to multiple testing. *Journal of the Royal Statistical Society: Series B (Methodological), 57*(1), 289–300.

Bonnington, C., Gaston, K. J., & Evans, K. L. (2014). Squirrels in suburbia: Influence of urbanisation on the occurrence and distribution of a common exotic mammal. *Urban Ecosystems, 17*(2), 533–546.

Broitman, D., & Koomen, E. (2015). Regional diversity in residential development: A decade of urban and peri-urban housing dynamics in the Netherlands. *Letters in Spatial and Resource Sciences, 8*(3), 201–217.

Chandan, M. C., Bharath, H. A., & Ramachandra, T. V. (2014). *Quantifying urbanisation using geospatial data and spatial metrics-a case study of madras*. Uttara Kannada, India: 13th–15th Nov.

Cochard, R., Maneepitak, S., & Kumar, P. (2014). Aquatic faunal abundance and diversity in relation to synthetic and natural pesticide applications in rice fields of Central Thailand. *International Journal of Biodiversity Science, Ecosystem Services & Management, 10*(2), 157–173.

Cooper, R. T. (2019). Projection of future precipitation extremes across the Bangkok Metropolitan Region. *Heliyon, 5*(5), e01678.

Díaz-Porras, D. F., Gaston, K. J., & Evans, K. L. (2014). 110 Years of change in urban tree stocks and associated carbon storage. *Ecology and Evolution, 4*(8), 1413–1422.

Estoque, R. C., & Murayama, Y. (2015). Intensity and spatial pattern of urban land changes in the megacities of Southeast Asia. *Land Use Policy, 48*, 213–222.

Evans, K. L., Newson, S. E., & Gaston, K. J. (2009). Habitat influences on urban avian assemblages. *Ibis, 151*(1), 19–39.

Geist, H. J., & Lambin, E. F. (2002). Proximate causes and underlying driving forces of tropical deforestation tropical forests are disappearing as the result of many pressures, both local and regional, acting in various combinations in different geographical locations. *BioScience, 52*(2), 143–150.

Güneralp, B., & Seto, K. C. (2013). Futures of global urban expansion: Uncertainties and implications for biodiversity conservation. *Environmental Research Letters, 8*(1), 014025.

Haaland, C., & van Den Bosch, C. K. (2015). Challenges and strategies for urban green-space planning in cities undergoing densification: A review. *Urban Forestry & Urban Greening, 14*(4), 760–771.

Hongtong, P. (2019). Deputy minister pitches new airport in Nakhon Pathom. [online]. December. [accessed 8 March 2021]. Available from: *Bangkok Post, 17* https://www.bangkokpost.com/thailand/general/1818219/deputy-minister-pitches-new-airport-in-nakhon-pathom.

Huang, K., Li, X., Liu, X., & Seto, K. C. (2019). Projecting global urban land expansion and heat island intensification through 2050. *Environmental Research Letters, 14*(11), 114037.

Hughes, A. C. (2017). Understanding the drivers of Southeast Asian biodiversity loss. *Ecosphere, 8*(1), e01624.

Jones, Z. F., & Bock, C. E. (2002). Conservation of grassland birds in an urbanizing landscape: A historical perspective. *The Condor, 104*(3), 643–651.

Kamoshita, A., Araki, Y., & Nguyen, Y. T. (2014). Weed biodiversity and rice production during the irrigation rehabilitation process in Cambodia. *Agriculture, Ecosystems & Environment, 194*, 1–6.

Kaspar, J., Kendal, D., Sore, R., & Livesley, S. J. (2017). Random point sampling to detect gain and loss in tree canopy cover in response to urban densification. *Urban Forestry & Urban Greening, 24*, 26–34.

Khamchiangta, D., & Dhakal, S. (2020). Time series analysis of land use and land cover changes related to urban heat island intensity: Case of Bangkok Metropolitan Area in Thailand. *Journal of Urban Management, 9*(4), 383–395.

Kummer, D. M., & Turner, B. L. (1994). The human causes of deforestation in Southeast Asia. *Bioscience, 44*(5), 323–328.

Lakatos, T., Chamberlain, D. E., Garamszegi, L. Z., & Batáry, P. (2022). No place for ground-dwellers in cities: A meta-analysis on bird functional traits. *Global Ecology and Conservation, 38*, e02217.

Lemoine-Rodríguez, R., MacGregor-Fors, I., & Muñoz-Robles, C. (2019). Six decades of urban green change in a neotropical city: A case study of Xalapa, Veracruz, Mexico. *Urban Ecosystems, 22*(3), 609–618.

Lin, B. B., Ossola, A., Alberti, M., Andersson, E., Bai, X., Dobbs, C., … Tan, P. Y. (2021). Integrating solutions to adapt cities for climate change. *The Lancet Planetary Health, 5*(7), e479–e486.

MacIvor, J. S. (2016). Building height matters: Nesting activity of bees and wasps on vegetated roofs. *Israel Journal of Ecology and Evolution, 62*(1–2), 88–96.

Moll, R. J., Cepek, J. D., Lorch, P. D., Dennis, P. M., Tans, E., Robison, T., … Montgomery, R. A. (2019). What does urbanization actually mean? A framework for urban metrics in wildlife research. *Journal of Applied Ecology, 56*(5), 1289–1300.

Morabito, M., Crisci, A., Guerri, G., Messeri, A., Congedo, L., & Munafò, M. (2021). Surface urban heat islands in Italian metropolitan cities: Tree cover and impervious surface influences. *Science of the Total Environment, 751*, 142334.

Myers, N., Mittermeier, R. A., Mittermeier, C. G., Da Fonseca, G. A., & Kent, J. (2000). Biodiversity hotspots for conservation priorities. *Nature, 403*(6772), 853–858.
Norton, B. A., Bending, G. D., Clark, R., Corstanje, R., Dunnett, N., Evans, K. L., … Warren, P. H. (2019). Urban meadows as an alternative to short mown grassland: Effects of composition and height on biodiversity. *Ecological Applications, 29*(6), e01946.
Nowak, D. J., Noble, M. H., Sisinni, S. M., & Dwyer, J. F. (2001). People and trees: Assessing the US urban forest resource. *Journal of Forestry, 99*(3), 37–42.
Parris, K. M. (2016). *Ecology of Urban Environment*. Chicester, United Kingdom: Wiley-Blackwell.
Pauleit, S., Ennos, R., & Golding, Y. (2005). Modeling the environmental impacts of urban land use and land cover change—A study in Merseyside, UK. *Landscape and Urban Planning, 71*(2–4), 295–310.
Pickett, S. T. (1989). Space-for-time substitution as an alternative to long-term studies. In *Long-term studies in ecology* (pp. 110–135). New York, NY: Springer.
Poapongsakorn, N., & Meethom, P. (2013). Impact of the 2011 floods, and flood management in Thailand. *ERIA Discussion Paper Series, 34*, 2013.
Ramamurthy, P., & Bou-Zeid, E. (2014). Contribution of impervious surfaces to urban evaporation. *Water Resources Research, 50*(4), 2889–2902.
Richards, D. R., Passy, P., & Oh, R. R. (2017). Impacts of population density and wealth on the quantity and structure of urban green space in tropical Southeast Asia. *Landscape and Urban Planning, 157*, 553–560.
Round, P. D., & Gardner, D. (2008). *The Birds of the Bangkok Area*. Bangkok, Thailand: White Lotus.
R Core Team. (2021). *R: A language and environment for statistical computing*. Vienna, Austria: R Foundation for Statistical Computing. https://www.R-project.org/.
Schneider, A., Mertes, C. M., Tatem, A. J., Tan, B., Sulla-Menashe, D., Graves, D., … Dastur, A. (2015). A new urban landscape in East-Southeast Asia, 2000–2010. *Environmental Research Letters, 10*(3), 034002.
Sejati, A. W., Buchori, I., & Rudiarto, I. (2018). The impact of urbanization to forest degradation in Metropolitan Semarang: A preliminary study. *IOP Conference Series: Earth and Environmental Science, 123*(1), Article 012011.
Seto, K. C., Fragkias, M., Güneralp, B., & Reilly, M. K. (2011). A meta-analysis of global urban land expansion. *PloS One, 6*(8), e23777.
Seto, K. C., Güneralp, B., & Hutyra, L. R. (2012). Global forecasts of urban expansion to 2030 and direct impacts on biodiversity and carbon pools. *Proceedings of the National Academy of Sciences, 109*(40), 16083–16088.
Sittipunt, C. (2022). Planting a million trees. [online]. 215 Chatchart's Policies. Latest update 3 May 2022. [Access 28 August 2022]. Available at https://www.chadchart.com/policy/6215eef94e43cd8b4760bc16/.
Sodhi, N. S., Koh, L. P., Brook, B. W., & Ng, P. K. (2004). Southeast Asian biodiversity: An impending disaster. *Trends in ecology & evolution, 19*(12), 654–660.
Sodhi, N. S., Koh, L. P., Clements, R., Wanger, T. C., Hill, J. K., Hamer, K. C., … Lee, T. M. (2010). Conserving Southeast Asian forest biodiversity in human-modified landscapes. *Biological Conservation, 143*(10), 2375–2384.
Song, Y., Aryal, J., Tan, L., Jin, L., Gao, Z., & Wang, Y. (2021). Comparison of changes in vegetation and land cover types between Shenzhen and Bangkok. *Land Degradation & Development, 32*(3), 1192–1204.
Song, W., Pijanowski, B. C., & Tayyebi, A. (2015). Urban expansion and its consumption of high-quality farmland in Beijing, China. *Ecological Indicators, 54*, 60–70.
Srivanit, M., Hokao, K., & Phonekeo, V. (2012). Assessing the impact of urbanization on urban thermal environment: A case study of Bangkok Metropolitan. *International Journal of Applied Science and Technology, 2*(7), 243–256.
Thailand. Ministerial Regulation. (1954). *Act Promulgating the Land Code*. Available at: http://web.krisdika.go.th/data/outsitedata/outsite21/file/Act_Promulgating_the_Land_Code_BE_2497_(1954).pdf(1954).pdf. [Accessed from 25 August 2022].
Thaiutsa, B., Puangchit, L., Kjelgren, R., & Arunpraparut, W. (2008). Urban green space, street tree and heritage large tree assessment in Bangkok, Thailand. *Urban Forestry & Urban Greening, 7*(3), 219–229.
Thanvisitthpon, N., Shrestha, S., & Pal, I. (2018). Urban flooding and climate change: A case study of Bangkok, Thailand. *Environment and Urbanization ASIA, 9*(1), 86–100.
Thaweepworadej, P., & Evans, K. L. (2022a). Avian species richness and tropical urbanisation gradient — Effects of woodland retention and human disturbance. *Ecological Applications, 37*, e2586.
Thaweepworadej, P., & Evans, K. L. (2022b). Species richness and ecosystem services of tree assemblages along an urbanisation gradient in a tropical mega-city: Consequences for urban design. *Urban Forestry & Urban Greening, 70*, 127527.
Thaweepworadej, P., & Evans, K. L. (2022c). Squirrel and tree-shrew responses along an urbanisation gradient in a tropical mega-city — reduced biodiversity, increased hybridisation of *Callosciurus* squirrels, and effects of habitat quality. *Animal Conservation*. https://doi.org/10.1111/acv.12797
Tuffour-Mills, D., Antwi-Agyei, P., & Addo-Fordjour, P. (2020). Trends and drivers of land cover changes in a tropical urban forest in Ghana. *Trees, Forests and People, 2*, 100040.
United Nations, Department of Economic and Social Affairs, Population Division. (2018). *World Urbanization Prospects: The 2018 Revision*. New York: United Nations.
United Nations, Department of Economic and Social Affairs, Population Division, 2019. World Population Prospects 2019, online edition. Available at: https://population.un.org/wpp/. [Accessed from 21 January 2021].
van Vliet, J. (2019). Direct and indirect loss of natural area from urban expansion. *Nature Sustainability, 2*(8), 755–763.
Wang, J., Zhou, W., Wang, J., & Qian, Y. (2019). From quantity to quality: Enhanced understanding of the changes in urban greenspace. *Landscape Ecology, 34*(5), 1145–1160.
Xu, G., Jiao, L., Liu, J., Shi, Z., Zeng, C., & Liu, Y. (2019). Understanding urban expansion combining macro patterns and micro dynamics in three Southeast Asian megacities. *Science of the Total Environment, 660*, 375–383.